# Standardized Threshold Approach using 3D Proton MR Spectroscopic Imaging in Prostate Cancer Localization of the Entire Prostate

**T. Scheenen[1], J. Futterer[1], S. Heijmink[1], H. Huisman[1], C. Hulsbergen-Van de Kaa[2], A. Witjes[3], J. Barentsz[1], and A. Heerschap[1]**

[1]Radiology (667), Radboud University Nijmegen Medical Centre, Nijmegen, Netherlands, [2]Pathology, Radboud University Nijmegen Medical Centre, Netherlands, [3]Urology, Radboud University Nijmegen Medical Centre, Netherlands

## Introduction

3D Proton MR spectroscopic imaging (MRSI) is a technique that provides metabolic information throughout the prostate gland. This information can be used to characterize prostate tissue, cancer aggressiveness and therapy evaluation [1]. With the wider range of therapeutic options (prostatectomy, brachytherapy, intensity modulated radiotherapy) for prostate cancer, accurate localization of the disease has become increasingly important. Prostate cancer has been shown to be characterized by a decreased signal of citrate proton spins and an increased signal of proton spins in choline-containing compounds. Therefore, a marker for cancer tissue is the choline + creatine / citrate ratio, commonly used in the peripheral zone of the prostate gland. However, thirty percent of prostate tumor foci are found in the central gland, where localization can be hampered by benign diseases and the presence of the ejaculatory ducts. In spectra of voxels containing these ducts increased intensities near the choline resonance can occur of phosphorylcholine [2], which could result in an apparent increased choline + creatine / citrate ratio by an unaware reader, and thereby a false positive finding of prostate cancer. Therefore, in this work we propose to adopt a standardized threshold approach [3] to values from healthy regions in either the central gland or the peripheral zone.

## Materials and methods

32 consecutive men with biopsy-proven and clinically localized prostate cancer underwent endorectal coil MR examinations prior to radical prostatectomy and at least 3 weeks after transrectal ultrasound-guided sextant biopsy. After T2-weighted fast spin echo imaging with an in plane resolution of 0.55 x 0.55-mm (TR 3500-4400 ms/ TE 132 ms, slice thickness 4 mm) in three orthogonal planes of the prostate and seminal vesicles, 3D MRSI of the entire prostate was performed with a 3D PRESS pulse sequence with optimized 180º pulses and an echo time of 120 ms for use on 1.5T Siemens Magnetom scanners [4]. Water and lipid signals are suppressed with two dual-frequency selective excitation pulses and crusher gradients. Nominal resolution of the spectroscopic voxels is 6x6x6 $mm^3$, which is enlarged by apodization of k-space for accurate localization and decreased voxel bleed. By using a short TR (650 ms) and an elliptical, weighted acquisition scheme the total acquisition time is between 10 and 12 minutes, depending on the exact number of phase encode steps and averages.

After time-domain filtering, zerofilling, automatic residual water removal and phasing, the integrals of creatine, choline and citrate from the individual spectra were determined with the Syngo software by an automated Gaussian curve fitting routine. Two radiologists and one spectroscopist, aware of the presence of prostate cancer, but blinded to all other clinical data, read the combined MRI and MRSI data of the patients onto a standardized scoring scheme (Fig. 1). The readers evaluated all voxels in one ROI, searching for the highest representative choline + creatine / citrate (CC/C) ratio in a ROI. After they found the highest ratio in a ROI the neighboring voxels were evaluated to validate this finding. The CC/C ratio of the representative voxels was calculated exactly and classification was performed on the basis of threshold values reported from the initial results of a multi-center trial [5] that uses the exact same acquisition parameters as used here. A zone-specific threshold approach is based on the mean values + one to five standard deviations of the CC/C ratio in either healthy peripheral zone or central gland (Table I). Assessment of the choline-to-creatine ratio was also included in the analysis: if the choline signal was more than twice the size of the creatine signal, an initial score of 2 or 3 was increased to 4. If the choline signal was less than twice the creatine signal, an initial score of 4 was set down to 3, and an initial score of 5 was brought down to 4. The readers were allowed to assign MR spectra as unusable if they showed substantial lipid contamination, poor spectral signal-to-noise ratio or baseline abnormalities.

After radical prostatectomy the prostates were fixed and sectioned at 4-mm interval in a plane parallel to the axial T2-weighted sequence. After separating the step sections into right and left halves all sections were routinely embedded in paraffin, sliced and stained. The presence and extent of cancer were outlined on the glass slide cover, and transferred to the standardized scoring scheme (Fig. 1). For nodules with a histopathologic volume greater than 0.50 $cm^3$, MRI and MRSI was correlated with the histopathologic conclusion. An ROI was called positive if tumor was present. The sensitivity, specificity, positive and negative predictive value and overall accuracy were determined by dichotomizing the readings: ROIs of 1 and 2 were considered normal prostate tissue while scores of 3 to 5 were considered malignant. ROI receiver operating characteristic (ROI-ROC) curves for tumor localization were calculated and the interobserver agreement was evaluated by using non-weighted kappa (κ) statistics (κ: 0.0-0.2 = poor agreement, 0.21-0.4 = fair agreement, 0.41-0.6 = moderate agreement, 0.61-0.8 = substantial agreement and 0.81-1.0 = near-perfect agreement [6])

| Rating | | peripheral zone | central gland |
|---|---|---|---|
| 1 | definitely benign tissue | ≤ 0.44 | ≤ 0.52 |
| 2 | probably benign tissue | 0.44 - 0.58 | 0.52 – 0.66 |
| 3 | possible malignant tissue | 0.58 - 0.72 | 0.66 – 0.80 |
| 4 | probably malignant tissue | 0.72 - 0.86 | 0.80 – 0.94 |
| 5 | definitely malignant tissue | > 0.86 | > 0.94 |

Table 1. CC/C Ratios for prostate tissue on a five-point scale, defined by the mean value of healthy tissue + one to five standard deviations.

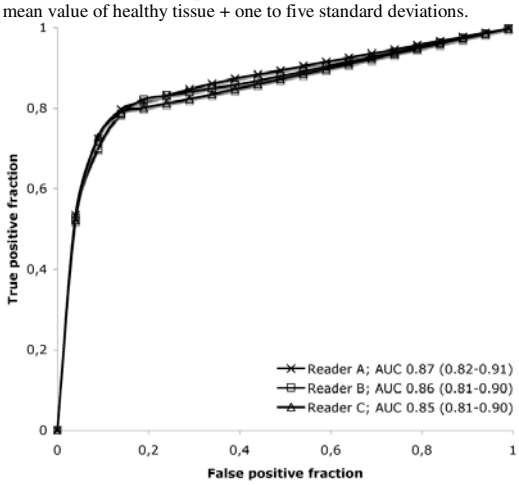


Figure 2. ROC curves and areas under the ROC curves (AUC) of prostate cancer localization using 3D $^1$H-MRSI for all three readers. No significant differences were found between readers.

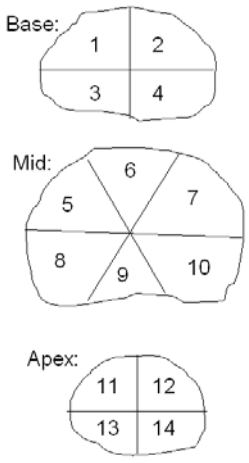


Figure 1. Standardized scoring scheme of a prostate. Both MR and histopathological data were transferred to this scoring form.

## Results and discussion

104 out of 448 ROIs (23%) were positive for prostate cancer, with 73% present in the peripheral zone and 27% in the central gland. A total of 64, 88 and 52 out of the 448 ROIs were assigned unusable for reader A, B and C, respectively, and were excluded in the further analysis. The overall localization accuracy using 3D MRSI was 85%, 84%, and 86% for reader A, B and C, respectively. For all three readers, the sensitivity was substantial (75% - 92%) and specificity was high (81% - 88%). Especially in the central gland the negative predictive value was high (i.e. 97% - 99%), however the positive predictive value ranged from 48% to 53%. No statistically significant differences were found when comparing results of the descriptive analysis obtained for the peripheral zone and central gland.

The ROI-ROC curves describing the results of 3D MRSI localization performance are presented in figure 2. The AUC for the entire prostate was 0.87 for reader A, 0.86 for reader B and 0.85 for reader C. The interobserver agreement was near-perfect (κ = 0.91) for reader A - C and moderate for reader pairs A – B (κ = 0.42) and B – C (κ = 0.54) using 3D MRSI in localizing prostate carcinoma.

## Conclusions

Our results indicate that a standardized zone-specific threshold approach in 3D $^1$H-MRSI can be applied with good accuracy and interobserver agreement for evaluation throughout the prostate. The quantitative nature of using metabolite ratios and zone-specific thresholds, resulted in high interobserver agreements. If data analysis was further automated, this technique could prove to be even less reader-dependent.

**References: 1.** Zakian KL *et al.* Radiology 2005; 234:804-814. **2.** Tomlins AM *et al.* BBA 1998; 1379: 367-380; **3.** Jung J *et al*. Radiology 2004; 233: 701-708; **4.** Scheenen TWJ *et al.* Magn Reson Med 2004;52:80-88; **5.** Scheenen TWJ *et al.* Proc. of 13th ISMRM, 2005; **6.** Rutter CM. Acad Radiol 2000; 7:413-419.